

# Nitrogen-Doped Carbon Nanotubes as an Effective Support of Heterogeneous Catalysts for Selective Alkene Oxidation

A. N. Suboch<sup>a,\*</sup>, V. Yu. Evtushok<sup>a</sup>, L. S. Kibis<sup>a</sup>, O. A. Kholdeeva<sup>a</sup>, and O. Yu. Podyacheva<sup>a</sup>

<sup>a</sup> Boreskov Institute of Catalysis, Siberian Branch, Russian Academy of Sciences, Novosibirsk, 630090 Russia

\*e-mail: arina@catalysis.ru

Received June 15, 2020; revised October 8, 2020; accepted October 29, 2020

**Abstract**—Nitrogen-doped carbon nanotubes (N-CNTs) with different degrees of nitrogen doping were synthesized. The effects of nitrogen in the N-CNTs on the hydrophilic–hydrophobic properties of carbon nanotubes and their activity in the decomposition of H<sub>2</sub>O<sub>2</sub> were studied. Various approaches to the surface modification of N-CNTs by alkyl groups were studied, and the high resistance of N-CNTs to alkylation was found. Heterogeneous catalysts based on the polyoxometallate [PO<sub>4</sub>{WO(O<sub>2</sub>)<sub>2</sub>}<sub>4</sub>]<sup>3-</sup> and N-CNTs with a low degree of nitrogen doping (≤1.8 at %) were successfully synthesized. The high efficiency of the catalysts in the liquid-phase reactions of selective oxidation of alkenes using H<sub>2</sub>O<sub>2</sub> as a green oxidizer was found, and the heterogeneous nature of catalysis was confirmed.

**Keywords:** carbon nanotubes, nitrogen doping, polyoxometallates, alkenes, liquid-phase oxidation

**DOI:** 10.1134/S0023158421020105

## INTRODUCTION

Epoxides are widely used as building blocks for basic and fine organic synthesis due to the special reactivity of an oxirane ring [1]. The oxidation of alkenes using various substances containing a peroxide group is one of the main methods for the preparation of epoxides [2]. The majority of synthetic approaches are based on the use of peracids [2] and alkyl hydroperoxides [3] as oxidants. However, the use of aqueous hydrogen peroxide as a green oxidizing agent is of significant economic and environmental interest [4–6]. On the homolytic activation of hydrogen peroxide, radicals are formed to direct the reaction along the allylic oxidation route. As a result, the selective epoxidation of alkenes with hydrogen peroxide can be carried out only in the presence of a catalyst that heterolytically activates hydrogen peroxide [4, 5].

Metal-oxygen clusters or polyoxometallates (POMs) are of great interest as catalysts for oxidative processes because they are thermodynamically stable to oxidation, structurally various, and capable of activating various oxidizing agents [6]. The tetranuclear phosphotungstate [PO<sub>4</sub>{WO(O<sub>2</sub>)<sub>2</sub>}<sub>4</sub>]<sup>3-</sup> (PW<sub>4</sub>), which is

also known as the Venturolo complex, has long been used as an active and selective homogeneous catalyst for the epoxidation of alkenes with hydrogen peroxide [7, 8]. However, the effective use of this active component requires its immobilization on the surface of an inert support, which exhibits high stability under conditions of an aggressive liquid reaction medium.

It is well known that carbon nanomaterials (CNMs) are promising in the design of hybrid inorganic composites for electronics, energy conversion and storage, molecular sensors, and catalysis [9]. Composites based on POMs and CNMs are actively studied as electrocatalysts for water splitting or redox reactions in fuel cells [10–13]. Conventional adsorption [12] and impregnation [14] are the main methods of POM immobilization on the surface of CNMs; however, more complicated methods, such as electrostatic bonding through functional groups previously introduced onto the surface of CNMs [10] or covalent bonding through organically modified POMs [13], are also used.

The doping of CNM structures with nitrogen atoms (N-CNM) provides additional possibilities for the immobilization of active centers. Nitrogen in CNMs is incorporated into pyridine-like (N<sub>py</sub>), pyrrole (N<sub>pyr</sub>), graphite-like (N<sub>g</sub>), and oxidized (N<sub>ox</sub>) structural positions [15–17]. The morphology of CNMs, the amount of nitrogen, and a ratio between its forms are the main factors influencing the functional properties of composites based on N-CNMs. Numerous works have demonstrated an increase in

**Abbreviations and designations:** CNTs, carbon nanotubes; N-CNTs, nitrogen-containing carbon nanotubes; POMs, polyoxometallates; PW<sub>4</sub>, the tetranuclear phosphotungstate [PO<sub>4</sub>{WO(O<sub>2</sub>)<sub>2</sub>}<sub>4</sub>]<sup>3-</sup>; N<sub>py</sub>, N<sub>pyr</sub>, N<sub>g</sub>, and N<sub>ox</sub>, pyridine-like, pyrrole, graphite-like, and oxidized structural positions, respectively; TG, thermogravimetry; DTA, differential thermal analysis; DSC, differential scanning calorimetry; TPO, temperature-programmed oxidation; XPS, X-ray photoelectron spectroscopy.

the catalytic activity of catalysts supported onto nitrogen-containing carbon nanofibers [15, 18, 19], carbon nanotubes (N-CNTs) [20, 21], mesoporous carbon [22, 23], etc. Recently, Evtushok et al. [24] reported the possibility of stable immobilization of POMs on N-CNTs. According to the experimental data, the conversion and selectivity of the synthesized catalyst were comparable to those of a homogeneous catalyst in the selective oxidation reaction of alkyl phenol to a corresponding alkyl *p*-benzoquinone with the use of hydrogen peroxide as an oxidizing agent.

The aim of this work was to study N-CNTs with different degrees of doping with nitrogen and to obtain an effective heterogeneous catalyst based on POMs and N-CNTs for the selective oxidation of various alkenes.

## EXPERIMENTAL

### *Materials*

Cyclooctene (98%) and cyclohexene (98%) were obtained from Fluka and passed through neutral alumina before use. Acetonitrile (Panreac, HPLC grade) was dried and stored with activated molecular sieves 4 Å. All other reagents and solvents were of high purity grade, and they were used without further purification. The concentration of H<sub>2</sub>O<sub>2</sub> (about 30 wt % in water) was determined by iodometry before use.

### *POM Synthesis*

The tetrahexylammonium salt of polyoxotungstate ((C<sub>7</sub>H<sub>15</sub>)<sub>4</sub>N)<sub>3</sub>[PO<sub>4</sub>{WO(O<sub>2</sub>)<sub>2</sub>}]<sub>4</sub>) was obtained according to a published procedure [25]. The purity of the compound was confirmed by IR spectroscopy and <sup>31</sup>P NMR spectroscopy.

### *CNT and N-CNT Synthesis*

Carbon nanotubes (CNTs) and nitrogen-containing carbon nanotubes (N-CNTs) were synthesized by the catalytic pyrolysis of ethylene or an ethylene–ammonia mixture on a Fe–Ni–Al<sub>2</sub>O<sub>3</sub> catalyst at 700°C [26, 27]. The concentration of ammonia in the mixture was varied from 10 to 60 vol %. To remove the catalyst from CNTs and N-CNTs, the materials were treated with concentrated hydrochloric acid for seven days with the subsequent boiling in 2 M HCl for 6 h. The samples were washed to remove chloride ions by repeated boiling in distilled water until the disappearance of a positive test for Cl<sup>−</sup>. The catalyst content decreased to 1–2 wt %. High-resolution microscopy showed that the remaining catalyst particles were in an encapsulated state and, accordingly, the washed carbon nanotubes were inert in the H<sub>2</sub>O<sub>2</sub> decomposition reaction. The washed samples were dried in air and then calcined in Ar at 170°C for 2 h. Before POM

immobilization, the N-CNTs were additionally dried in a vacuum at 100°C.

### *N-CNT Alkylation with CH<sub>3</sub>I*

A 200-mg weighed portion of 1.8 at % N-CNTs (1.8% N-CNTs) was placed in a high-pressure glass vessel with a screw cap; 50 μL of CH<sub>3</sub>I was added, and the contents were left under stirring for 48 h at 25°C. Then, the temperature was raised to 50°C, and the contents were stirred for another 8 h. The carbon nanotubes were filtered off, washed with a small amount of diethyl ether, and dried in a flow of air.

### *N-CNT Alkylation with C<sub>4</sub>H<sub>9</sub>Br*

A 200-mg weighed portion of 4.8% at % N-CNTs (4.8% N-CNTs) was placed in a high-pressure glass vessel with a screw cap; 3 mL of toluene and 1 mL of C<sub>4</sub>H<sub>9</sub>Br were added, and the mixture was stirred for 24 h at 120°C. Then, the sample was filtered off, washed with a small amount of diethyl ether, and dried in a flow of air.

### *N-CNT Alkylation with C<sub>4</sub>H<sub>9</sub>Li*

A 200-mg weighed portion of 4.8% at % N-CNTs was placed in a flask with 5 mL of a concentrated solution of KOH in ethanol; then, the N-CNTs were filtered off and washed with ethanol. After rapid air drying, the sample was dried in a vacuum at 100°C and the flask was filled with argon. In a flow of argon, 3 mL of hexane and 400 μL of a 2.5 M solution of C<sub>4</sub>H<sub>9</sub>Li in hexane were added to the N-CNTs at room temperature with stirring, and the mixture was allowed to stand for 24 h. Then, 100 μL of C<sub>4</sub>H<sub>9</sub>Br was added to the mixture, and it was kept for another 48 h. The reaction mixture was quenched with ethanol, and the N-CNTs were filtered off, washed with a small amount of diethyl ether, and dried in air.

### *POM Immobilization*

The adsorption of PW<sub>4</sub> on CNTs and N-CNTs from a MeCN solution was carried out at room temperature. To increase the adsorption capacity, HClO<sub>4</sub> (1 equiv with respect to PW<sub>4</sub>) was added on the adsorption onto N-CNTs; the adsorption onto CNTs was performed without adding HClO<sub>4</sub>. The completion of the adsorption process was monitored using UV–visible spectroscopy. The resulting solid material was separated by filtration, washed three times with MeCN, and dried in a vacuum at 60°C.

### *H<sub>2</sub>O<sub>2</sub> Decomposition*

A carbon support (10 mg) was placed in a glass reactor containing 5 mL of MeCN, and then 50 μL of

**Table 1.** The total nitrogen content of N-CNTs and the percentages of nitrogen in different electronic states

[NH <sub>3</sub> ], vol %	[N <sub>total</sub> ], at %	N <sub>Py</sub> /N <sub>total</sub> , %	N <sub>Pyr</sub> /N <sub>total</sub> , %	N <sub>Q</sub> /N <sub>total</sub> , %	N <sub>Ox</sub> /N <sub>total</sub> , %	N <sub>N<sub>2</sub></sub> /N <sub>total</sub> , %
0	0	0	0	0	0	0
10	0.8	23	10	40	10	17
25	1.8	16	13	33	11	26
40	3.1	18	10	32	13	27
60	4.8	27	18	25	10	20

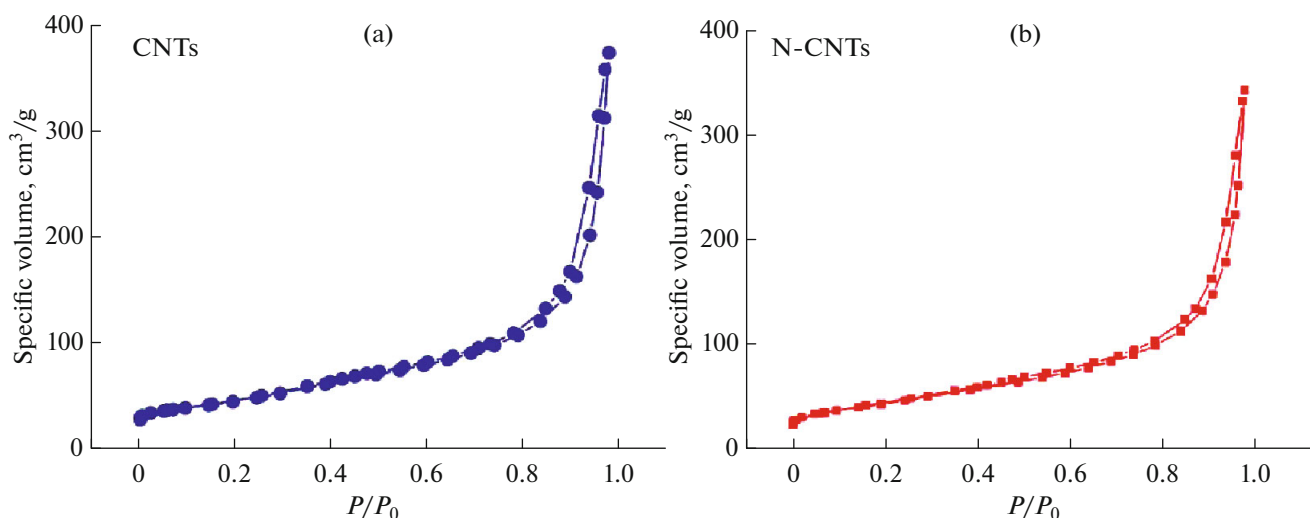
11 M H<sub>2</sub>O<sub>2</sub> was added. The reaction mixture was vigorously stirred at 50°C, and the samples of the solution (300 μL) were taken at regular intervals with a syringe. The H<sub>2</sub>O<sub>2</sub> concentration was determined by titration with a 0.002 M solution of KMnO<sub>4</sub>. The initial rates of decomposition of H<sub>2</sub>O<sub>2</sub>  $W_0$  were found from the slopes of the initial sections of kinetic curves.

#### Catalytic Oxidation and Product Analysis

Catalytic experiments were carried out in thermostatically controlled glass vessels with vigorous stirring (500 rpm). Typical conditions for oxidation reactions were the following: 0.1 M alkene, 0.1–0.2 M H<sub>2</sub>O<sub>2</sub>, 10 mg of 15 wt % PW<sub>4</sub>/N-CNT, 1 mL of MeCN, and 50°C. The reaction conditions were chosen based on the results of earlier studies of heterogeneous catalysts based on PW<sub>4</sub> [24, 25]. Reactions started with the addition of H<sub>2</sub>O<sub>2</sub>. The reaction products were identified by gas chromatography–mass spectrometry (GC–MS) and <sup>1</sup>H NMR spectroscopy and quantitatively determined on a gas chromatograph using biphenyl as an internal standard.

#### Physicochemical Research Methods

The reaction mixtures were analyzed using a Khromos GKh-1000 gas chromatograph (Khromos Engineering, Russia) equipped with a flame ionization detector and a BPX5 quartz capillary column (30 m × 0.25 mm). The <sup>31</sup>P NMR spectra were recorded on an AVANCE-400 spectrometer (Bruker, Germany) at 161.67 MHz. The chemical shift of P was determined relative to 85% H<sub>3</sub>PO<sub>4</sub>. The UV–visible spectra were recorded on a Cary 60 spectrophotometer (Varian, the United States). The X-ray photoelectron spectroscopy (XPS) spectra were measured on an ES-300 photoelectron spectrometer (KRATOS Analytical, the United Kingdom) using AlK $\alpha$  radiation ( $h\nu = 1486.6$  eV). The energy scale of the spectrometer was calibrated using the Au 4f<sub>7/2</sub> and Cu 2p<sub>3/2</sub> spectra of gold and copper the binding energies of which were taken 84.0 and 932.7 eV, respectively. The nitrogen content of N-CNTs was determined as the ratio N/C (at %), which was calculated from the intensities of the corresponding spectral lines (N1s and C1s) taking into account corrections for the atomic sensitivity factors of either of the elements. The texture characteristics were studied using the adsorption of nitrogen at 77 K on an ASAP-2400 specific surface area analyzer (Micrometrics, the United States) with preliminary

**Fig. 1.** Isotherms of N<sub>2</sub> adsorption on (a) CNTs and (b) 4.8% N-CNTs at 77 K.

**Table 2.** Data on the quantitative surface composition of the sample modified with  $\text{CH}_3\text{I}$  and the initial N-CNTs according to XPS data

Sample	Concentration, at %						$N_{\text{at}}/C_{\text{at}}$ , %
	C	O	N	Cl	Fe	I	
N-CNTs- $\text{CH}_3\text{I}$	95.5	2.4	1.8	0.1	0.1	0.1	1.9
N-CNTs	95.6	2.4	1.8	0.1	0.1	0	1.9

training of the samples in a vacuum at  $200^\circ\text{C}$ . The moisture capacity of carbon nanotubes was found by a standard gravimetric method. For this purpose, a solvent (water or acetone) was added to a certain weighed portion of the sample with stirring until wet, and the resulting sample was weighed. The added amount of liquid referred to the sample weight was recorded as the moisture capacity of the sample.

The thermal analysis (TPO) of the samples was performed using an STA 449 C Jupiter synchronous thermoanalyzer (NETZSCH, Germany). The sample was placed in a corundum crucible without a lid in an atmosphere of air. The air flow rate into the sample chamber was 30 mL/min. Helium was supplied to the weighing block at a flow rate of 20 mL/min. The sample was first heated at a rate of 2 K/min from room temperature to  $50^\circ\text{C}$  and kept at this temperature for 30 min; then, a temperature-programmed heating to  $1000^\circ\text{C}$  was carried out at a rate of 5 K/min.

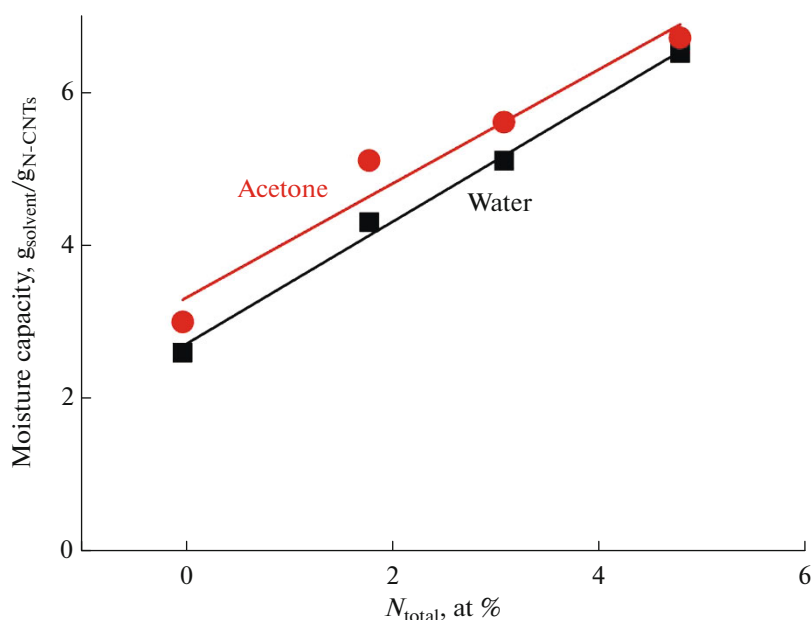
## RESULTS AND DISCUSSION

### *Physicochemical Properties of N-CNTs*

The concentrations of nitrogen and the fractions of various nitrogen species in N-CNTs were determined using XPS. Table 1 indicates that an increase in the concentration of ammonia in the reaction mixture from 10 to 60 vol % was accompanied by an increase in the nitrogen content of N-CNTs from 0.8 to 4.8 at %. In all cases, nitrogen was incorporated into standard structural positions ( $N_{\text{Py}}$ ,  $N_{\text{Pyr}}$ , and  $N_{\text{Q}}$ ), and the relative contribution of  $N_{\text{Q}}$  decreased from 40 to 25% as the degree of doping was increased.

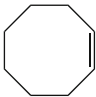
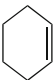
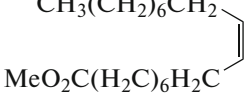
The study of the textural characteristics of carbon nanotubes showed that N-CNTs, like CNTs, were mesoporous materials, as indicated by the presence of a capillary-condensation hysteresis in the adsorption isotherms (Fig. 1). The CNT/N-CNT specific surface areas, average pore sizes, and pore volumes were 150–200  $\text{m}^2/\text{g}$ , 12–18 nm, and 0.5–0.9  $\text{cm}^3/\text{g}$ , respectively.

The ability of carbon nanotubes to adsorb various solvents was analyzed on the basis of data on the moisture holding capacity of the materials for water and acetone. As can be seen in Fig. 2, the moisture capacity of N-CNTs for both water and acetone increased with the nitrogen content to reach a maximum value of 6 mL/g. The found moisture capacity values are much higher than the pore volumes of carbon nanotubes determined based on nitrogen adsorption. It is most likely that nitrogen centers increase the hydrophilicity of a carbon surface to result in the volumetric filling of the inner channels of tubes [29, 30]. An increase in moisture capacity with the nitrogen content of N-



**Fig. 2.** Dependence of the moisture capacity of N-CNTs for water and acetone on the nitrogen content.

**Table 3.** Oxidation of various alkenes with hydrogen peroxide in the presence of PW<sub>4</sub>/N-CNTs catalysts\*

Alkene	No.	Catalyst	H <sub>2</sub> O <sub>2</sub> , M	Time, h	Conversion, %	Selectivity for epoxide, %
	1	15 wt % PW <sub>4</sub> /0.8% N-CNTs	0.2	3	90	95
	2	15 wt % PW <sub>4</sub> /1.8% N-CNTs	0.2	2	95	99
	3	15 wt % PW <sub>4</sub> /0.8% N-CNTs	0.1	4	55	43
	4	5 wt % PW <sub>4</sub> /CNTs**	0.1	4	66	79
$\text{CH}_3(\text{CH}_2)_6\text{CH}_2$ 	5	15 wt % PW <sub>4</sub> /0.8% N-CNTs	0.2	4	80	80
	6	5 wt % PW <sub>4</sub> /CNTs**	0.1	4	85	85

\* Reaction conditions: alkene, 0.1 M; PW<sub>4</sub>/N-CNTs catalyst, 10–30 mg (7 μmol of PW<sub>4</sub>); CH<sub>3</sub>CN or dimethyl carbonate, 1 mL; 50°C.

\*\* Solvent: dimethyl carbonate.

CNTs can have a positive effect on the POM amount adsorbed on the surface.

Thermal analysis showed that CNTs and 4.8% N-CNTs contained no amorphous carbon impurities because the DTA curves had only one maximum in the region of 500–600°C. The observed shift of a maximum toward low temperatures by 140°C (Fig. 3) indicates a decrease in the thermal stability of N-CNTs, as compared to that of CNTs, due to their greater defectiveness [27].

In the framework of this work, we studied a possibility of the alkylation of nitrogen-containing carbon nanotubes with various reagents. The surface modification of N-CNTs with alkyl groups can increase the surface hydrophobicity; in turn, this can affect the selectivity of catalytic epoxidation reactions of alkenes with hydrogen peroxide in the presence of POM/N-CNT catalysts. Because the selectivity of epoxidation on POM/N-CNTs mainly depends on the rate of a side reaction of epoxy ring opening, surface hydrophobization will decrease the surface concentration of water and decrease the rate of hydrolytic ring opening thus increasing the yield of epoxides. In the case of N-CNTs, the above modification can be carried out by the alkylation of N groups on the surface of the N-CNTs using various alkylating agents, for example, CH<sub>3</sub>I and C<sub>4</sub>H<sub>9</sub>Br. It is assumed that pyridine-like nitrogen groups will be the most reactive in this process due to their high nucleophilicity. By analogy with pyrrole, pyrrole groups can also be accessible for alkylation, but after treatment with a base and deprotonation.

To modify the surface of 1.8% N-CNTs with methyl groups, methyl iodide CH<sub>3</sub>I was chosen as a methylating reagent, which can almost quantitatively methylate pyridine under mild conditions, because the fraction of pyridine-like N among the N groups in the N-CNTs was approximately 20% (Table 1). How-

ever, according to the XPS data (Fig. 4), the reaction of N-CNTs with a twofold excess of CH<sub>3</sub>I did not lead to surface modification with alkyl groups. The signal intensity of N<sub>py</sub> (398.4 eV) did not change after the reaction. In addition, each pyridinium N<sup>+</sup>–Me group formed should correspond to the counterion I<sup>–</sup>, which was detected only in trace amounts according to the XPS data (Table 2).

The next step was an attempt to use more severe conditions for the alkylation of N-CNTs, but the low boiling point of CH<sub>3</sub>I makes it difficult to carry out the process at higher temperatures. On this basis, 1-bromobutane C<sub>4</sub>H<sub>9</sub>Br was chosen to modify the surface of 4.8% N-CNTs [31]. The alkylation reaction of N-CNTs was carried out in a toluene/bromobutane mixture with a tenfold excess of bromobutane with respect to the nitrogen of N-CNTs. TPO was used to analyze the surface state because the elimination of butyl groups in a temperature range of 100–250°C with a corresponding weight loss of ~10% should be observed upon the heating of N-CNTs modified with these groups. However, the thermogram of N-CNTs after the reaction did not exhibit a step of weight loss at these temperatures, and the DTA curve also did not have a corresponding maximum (Fig. 5).

According to TPO data, the alkylation of pyrrole nitrogen groups after deprotonation with a strong base and the use of C<sub>4</sub>H<sub>9</sub>Li to modify the N-CNT surface due to nucleophilic substitution also did not lead to the expected result. This may be due to the accessibility of nitrogen centers to the reagent. Thus, regardless of the approach used, N-CNTs exhibited high resistance to alkylation, and further research is required to develop an effective method for the alkylation of the N groups of N-CNTs.

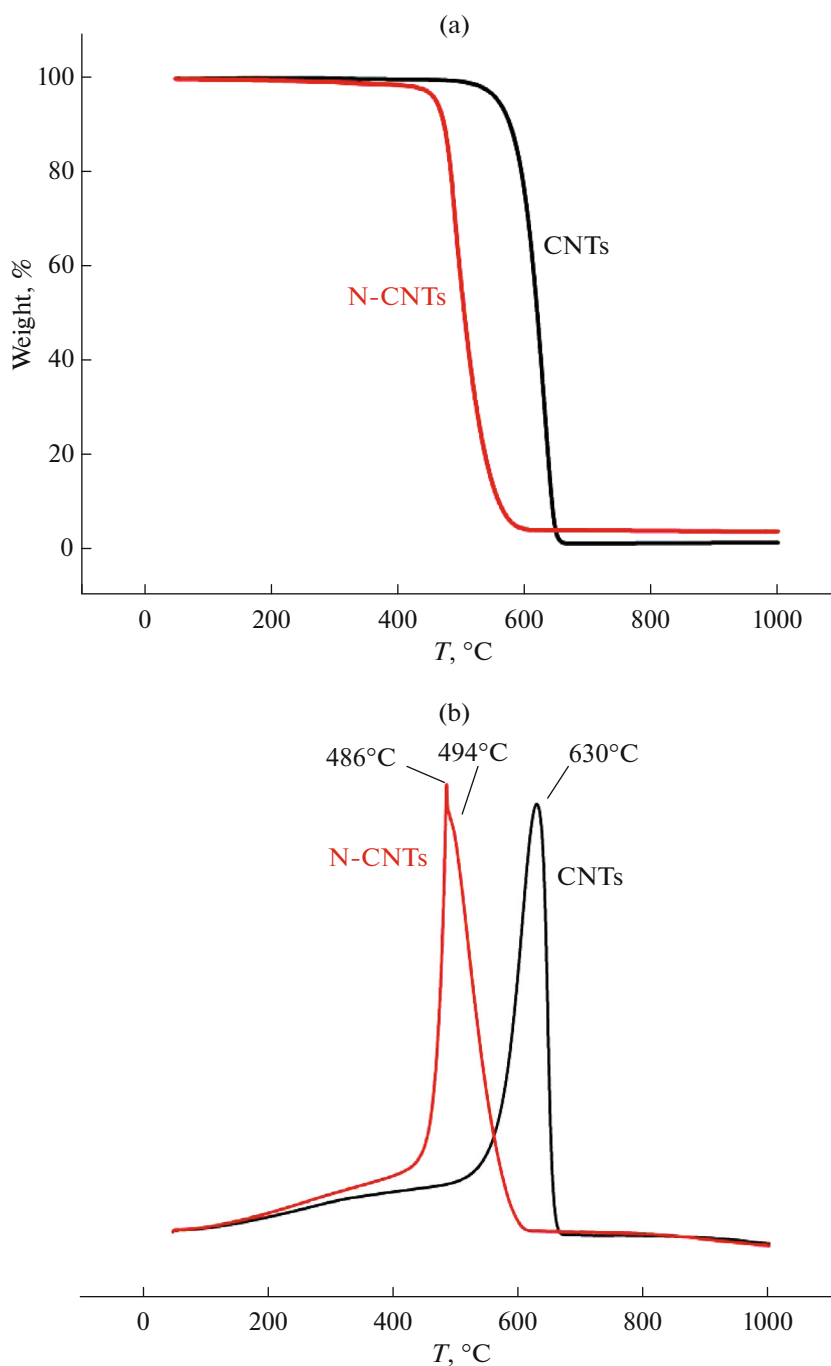


**Fig. 3.** (a) TG and (b) DTA curves for CNTs and 4.8% N-CNTs.

#### *Activity of the 15 wt % $PW_4$ /N-CNTs Catalyst*

Earlier, Evtushok et al. [24] found that nitrogen-containing tubes with the lowest nitrogen content are the most effective supports in the series 1.8% N-CNTs–4.8% N-CNTs. It was found that the rate of the unproductive reaction of  $H_2O_2$  decomposition increased with the degree of doping with nitrogen. To confirm the higher efficiency of N-CNTs with low nitrogen content, we used 0.8% N-CNTs as a support

for  $PW_4$  in this work. As can be seen in Fig. 6, the rate of decomposition of  $H_2O_2$  decreased by a factor of more than 2 as the nitrogen content was decreased from 1.8 to 0.8%.

The  $PW_4$ /N-CNTs catalysts were prepared by the adsorption of  $PW_4$  from a solution in MeCN on N-CNTs in accordance with a previously described procedure [24]. In the course of the sample preparation of 15 wt %  $PW_4$ /0.8% N-CNTs and, for comparison,

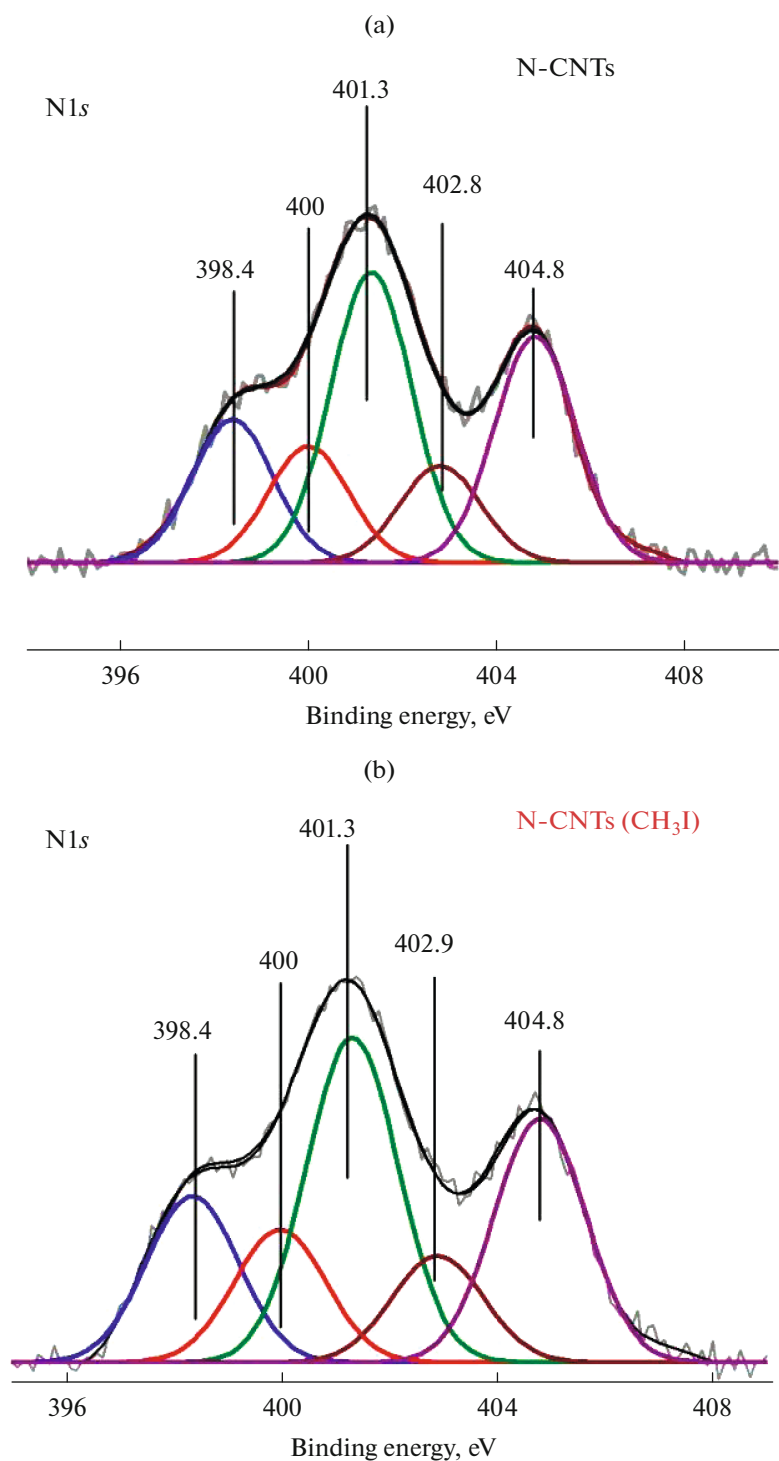


**Fig. 4.** N1s spectra of the 1.8% N-CNTs sample (a) before and (b) after methylation.

15 wt %  $\text{PW}_4/1.8\%$  N-CNTs, 1 equiv of  $\text{HClO}_4$  was added. Acid addition was not used to obtain the 5 wt %  $\text{PW}_4/\text{CNTs}$  catalyst.

The catalytic performance of 15 wt %  $\text{PW}_4/0.8\%$  N-CNTs was studied in the epoxidation reactions of various alkenes with a 30% aqueous solution of  $\text{H}_2\text{O}_2$ ,

and Table 3 summarizes these characteristics in comparison with those of other catalysts. The 15 wt %  $\text{PW}_4/0.8\%$  N-CNTs catalyst was slightly inferior to the 15 wt %  $\text{PW}_4/1.8\%$  N-CNTs catalyst in terms of conversion and selectivity in the oxidation of cyclooctene (Table 3, Nos. 1 and 2). However, the former sample

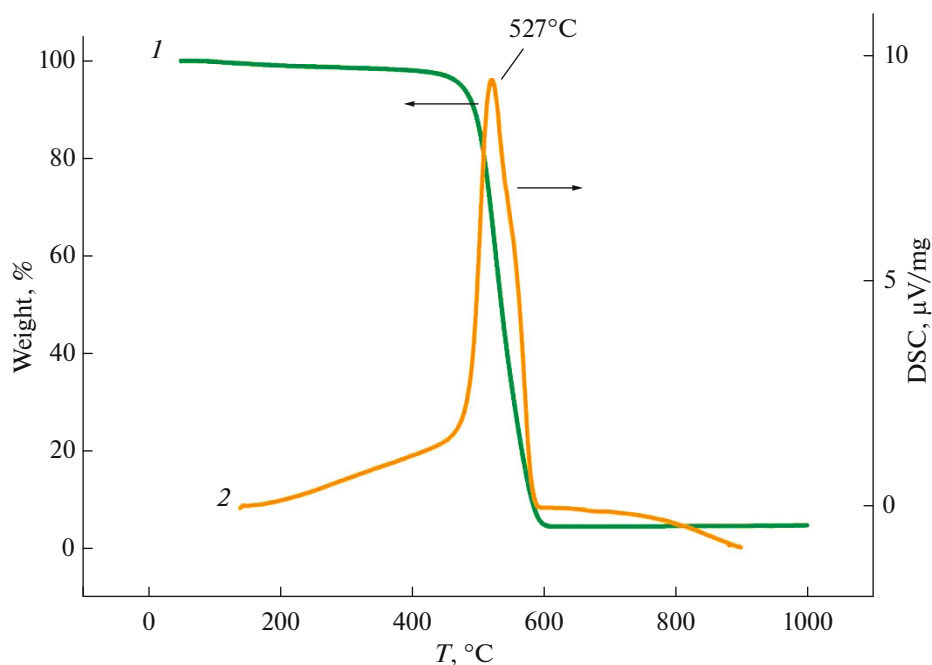


Fig. 5. (1) TG and (2) DTA curves for the 4.8% N-CNTs sample treated with bromobutane.

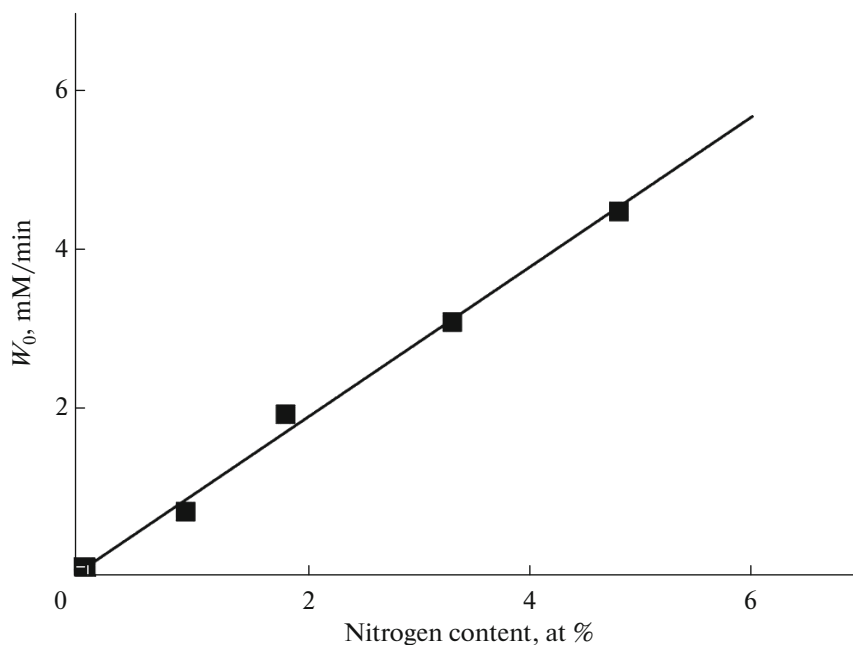
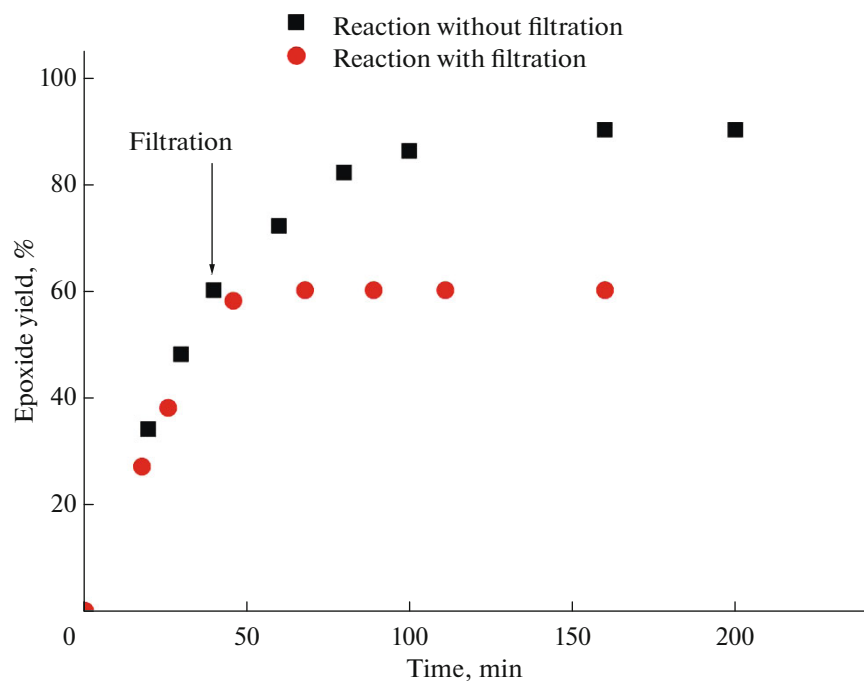


Fig. 6. Effect of the nitrogen content of N-CNTs on the initial rate of  $\text{H}_2\text{O}_2$  decomposition. Reaction conditions: 10 mg of CNTs, 0.11 M  $\text{H}_2\text{O}_2$ , 5 mL of  $\text{CH}_3\text{CN}$ , and  $50^{\circ}\text{C}$ .

demonstrated a 15% higher efficiency of  $\text{H}_2\text{O}_2$  utilization due to a smaller amount of nitrogen in it, as found upon the determination of  $\text{H}_2\text{O}_2$  amounts in the reaction mixtures at equal reaction times. This fact confirms the assumption that N-CNTs with a low degree of doping are optimal supports for the  $\text{PW}_4$  catalyst.

In the oxidation of cyclohexene and methyl oleate, the 15 wt %  $\text{PW}_4/0.8\%$  N-CNTs catalyst demonstrated moderate selectivity (43–80%) and conversion (55–80%) (Table 3, Nos. 3 and 5), and it was inferior to the acid-free 5 wt %  $\text{PW}_4/\text{CNTs}$  catalyst in selectivity (Table 3, Nos. 4 and 6). The analysis of reaction





**Fig. 7.** Hot filtration test in the epoxidation reaction of cyclooctene in the presence of 15 wt %  $\text{PW}_4/0.8\%$  N-CNTs. Reaction conditions: 0.1 M cyclooctene, 10 mg of the catalyst, 0.1 M  $\text{H}_2\text{O}_2$ , 1 mL of  $\text{CH}_3\text{CN}$ , and  $50^\circ\text{C}$ .

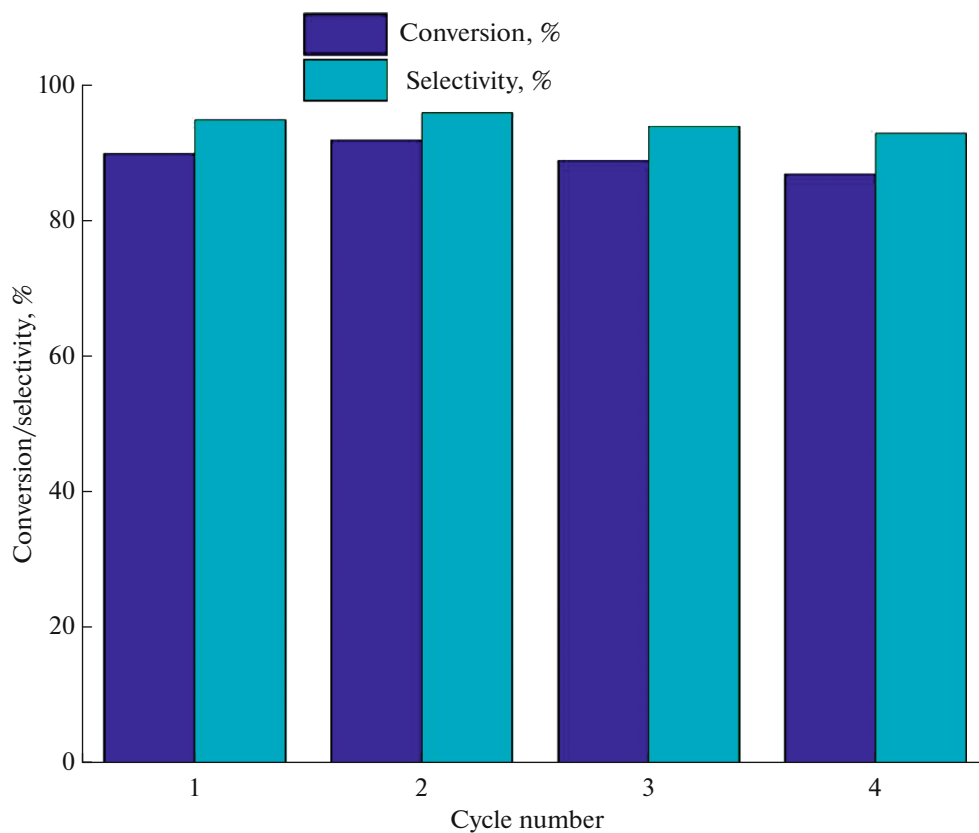


**Fig. 8.** Activity and selectivity of the 15 wt %  $\text{PW}_4/0.8\%$  N-CNT catalyst in four cycles of the cyclooctene epoxidation reaction. Reaction conditions: 0.1 M cyclooctene, 10 mg of the catalyst, 0.2 M  $\text{H}_2\text{O}_2$ , 1 mL of  $\text{CH}_3\text{CN}$ ,  $50^\circ\text{C}$ , and 240 min.

products showed that the lower selectivity of the 15 wt %  $\text{PW}_4/0.8\%$  N-CNTs catalyst for epoxide in the oxidation of cyclohexene was related to the formation of a large amount of the corresponding diol. Previously, it was found that the activity of  $\text{PW}_4/\text{CNTs}$  heterogeneous catalysts in epoxidation reactions increases with the amount of an  $\text{HClO}_4$  acid used for the immobilization of  $\text{PW}_4$ , whereas the selectivity in the epoxidation of alkenes, whose epoxides are sensitive to acid-catalyzed epoxy ring opening, decreases [25].

The hot filtration test confirmed the heterogeneous nature of catalysis (Fig. 7). This conclusion is based on the observed zero conversion of a substrate after the removal of the catalyst from the reaction medium. The strong immobilization of the active component on the surface of N-CNTs was found in cycling experiments, in which a catalyst sample was reactivated by heating at  $50^\circ\text{C}$  in a vacuum between cycles. With the use of 15 wt %  $\text{PW}_4/0.8\%$  N-CNTs in four reaction cycles of cyclooctene epoxidation, no significant drops in conversion (90 vs. 87%) and selectivity (95 vs. 93%) were found (Fig. 8). It should be noted that the resulting mesoporous 15 wt %  $\text{PW}_4/0.8\%$  N-CNTs catalyst is able to participate in the oxidation of bulky alkenes, such as cyclooctene or cyclohexene, in contrast to a well-known microporous titanium silicate catalyst TS-1 for the selective oxidation of alkenes with hydrogen peroxide. It is well known that the use of TS-1 without diffusion hindrances is limited to small alkenes such as propene [32, 33]. In addition, in the case of mesoporous titanium silicates, rapid catalyst deactivation in three to four cycles with the use of aqueous  $\text{H}_2\text{O}_2$  as an oxidizing agent is a problem, which is associated with Ti leaching in the course of the reaction, loss of the hierarchical structure, or the oligomerization of active centers [34]. In turn, the Ti-MMM-2 catalyst, which is stable in the epoxidation of alkenes with aqueous  $\text{H}_2\text{O}_2$ , is less active and selective in the epoxidation of cyclooctene than 15 wt %  $\text{PW}_4/0.8\%$  N-CNTs under comparable catalysis conditions. Thus, in the presence of Ti-MMM-2, the conversion of cyclooctene after a 24-h reaction was only 12% with 65% selectivity for epoxide formation [35]. Therefore, the above comparison shows that the use of N-CNTs as the effective support of a heterogeneous catalyst for selective oxidation of a wide range of different alkenes is promising.

## CONCLUSIONS

The synthesized N-CNTs with various degrees of nitrogen doping were studied as supports of a heterogeneous catalyst for the selective oxidation of alkenes. We demonstrated that the affinity for various solvents increased with the nitrogen content of the N-CNTs and the rate of the unproductive decomposition of  $\text{H}_2\text{O}_2$  increased by a factor of 5. With the use of  $\text{CH}_3\text{I}$ , 1-bromobutane ( $\text{C}_4\text{H}_9\text{Br}$ ), and  $\text{C}_4\text{H}_9\text{Li}$ , we found a

high resistance of N-CNTs to alkylation as a means of increasing the hydrophobicity of a carbon surface. The use of the most hydrophobic N-CNTs with a low degree of doping with nitrogen ( $\leq 1.8\%$ ) allowed us to perform strong immobilization of  $\text{PW}_4$  on the surface of carbon nanotubes. The resulting catalysts exhibited high activity and selectivity in the epoxidation reaction of cyclooctene, and they can be used repeatedly without a significant decrease in performance characteristics.

## ACKNOWLEDGMENTS

We are grateful to O.A. Nikolaeva for studying the samples by a TPO method.

## FUNDING

This work was supported by the Russian Foundation for Basic Research (grant no. 18-33-00764) and the Ministry of Science and Higher Education (project no. AAAA-A17-117041710084-2). The studies were carried out using the equipment of the Center of Collective Use "National Center for Catalyst Research."

## CONFLICT OF INTEREST

The authors have no conflicts of interest.

## REFERENCES

1. Sienel, G., Rieth, R., and Rowbottom, K.T., *Ullmann's Encyclopedia of Industrial Chemistry*, 2000, vol. 13, p. 139.
2. Swern, D., *Organic Peroxides, Vol. II*, New York: Wiley-Interscience, 1971, p. 963.
3. *Fine Chemicals through Heterogeneous Catalysis*, Sheldon, R.A. and van Bekkum, H., Eds., Wiley: Weinheim, 2001, p. 636.
4. Jones, C.W., *Applications of Hydrogen Peroxide and Derivatives*, Cambridge: Royal Society of Chemistry, 1999, p. 264.
5. *Catalytic Oxidations with Hydrogen Peroxide as Oxidant*, Strukul, G., Ed., Berlin: Springer, 2013, p. 286.
6. Hill, C.L. and Prosser-McCartha, C.M., *Coord. Chem. Rev.*, 1995, vol. 143, p. 407.
7. Venturello, C., D'Aloisio, R., Bart, J.C.J., and Ricci, M., *J. Mol. Catal.*, 1985, vol. 32, no. 1, p. 107.
8. Panicheva, L.P., Meteleva, G.P., Berlina, O.V., and Panichev, S.A., *Pet. Chem.*, 2006, vol. 46, no. 6, p. 422.
9. Eder, D., *Chem. Rev.*, 2010, vol. 110, p. 1348.
10. Toma, F.M., Sartorel, A., Iurlo, M., Carraro, M., Parrisse, P., Maccato, C., Rapino, S., Gonzalez, B.R., Amenitsch, H., Da, RosT., Casalis, L., Goldoni, A., Marcaccio, M., Scorrano, G., Scoles, G., Paolucci, F., Prato, M., and Bonchio, M., *Nat. Chem.*, 2010, vol. 2, p. 826.
11. Guo, S.-X., Liu, Y., Lee, C.-Y., Bond, A., Zhang, M.J., Geletii, Y.V., and Hill, C.L., *Energy Environ. Sci.*, 2013, vol. 6, p. 2654.

12. Kawasaki, N., Wang, H., Nakanishi, R., Hamanaka, S., Kitaura, R., Shinohara, H., Yokoyama, T., Yoshikawa, H., and Awaga, K., *Angew. Chem., Int. Ed.*, 2010, vol. 50, p. 3471.
13. Ji, Y., Huang, L., Hu, J., Streb, C., and Song, Y.-F., *Energy Environ. Sci.*, 2015, vol. 8, p. 776.
14. Wang, R., Yu, F., Zhang, G., and Zhao, H., *Catal. Today*, 2010, vol. 150, p. 37.
15. Podyacheva, O.Yu. and Ismagilov, Z.R., *Catal. Today*, 2015, vol. 249, p. 12.
16. Arrigo, R., Schuster, M.E., Xie, Z., Yi, Y., Wowsnick, G., Sun, L.L., Hermann, K.E., Friedrich, M., Kast, P., Hävecker, M., Knop-Gericke, A., and Schlögl, R., *ACS Catal.*, 2015, vol. 5, p. 2740.
17. Inagaki, M., Toyoda, M., Soneda, Y., and Morishita, T., *Carbon*, 2018, vol. 132, p. 104.
18. Zacharska, M., Podyacheva, O.Y., Kibis, L.S., Boronin, A.I., Senkovskiy, B.V., Gerasimov, E.Y., Taran, O.P., Ayusheev, A.B., Parmon, V.N., Leahy, J.J., and Bulushev, D.A., *ChemCatChem*, 2015, vol. 7, no. 18, p. 2910.
19. Ayusheev, A.B., Taran, O.P., Seryak, I.A., Podyacheva, O.Y., Descorme, C., Besson, M., Kibis, L.S., Boronin, A.I., Romanenko, A.I., Ismagilov, Z.R., and Parmon, V.N., *Appl. Catal., B*, 2014, vol. 146, p. 177.
20. Arrigo, R., Schuster, M.E., Xie, Z.L., Yi, Y.M., Wowsnick, G., Sun, L.L., Hermann, K.E., Friedrich, M., Kast, P., Hävecker, M., Knop-Gericke, A., and Schlögl, R., *ACS Catal.*, 2015, vol. 5, no. 5, p. 2740.
21. Suslova, E.V., Savilov, S.V., Egorov, A.V., and Lunin, V.V., *Kinet. Catal.*, 2019, vol. 60, p. 87.
22. Bulushev, D.A., Zacharska, M., Shlyakhova, E.V., Chuvilin, A.L., Guo, Y.N., Beloshapkin, S., Okotrub, A.V., and Bulusheva, L.G., *ACS Catal.*, 2016, vol. 6, no. 2, p. 681.
23. He, L., Weniger, F., Neumann, H., and Beller, M., *Angew. Chem., Int. Ed.*, 2016, vol. 55, no. 41, p. 12582.
24. Evtushok, V.Yu., Suboch, A.N., Podyacheva, O.Yu., Stonkus, O.A., Zaikovskii, V.I., Chesalov, Yu.A., Kibis, L.S., and Kholdeeva, O.A., *ACS Catal.*, 2018, vol. 8, p. 1297.
25. Evtushok, V.Yu., Ivanchikova, I.D., Podyacheva, O.Yu., Stonkus, O.A., Suboch, A.N., Chesalov, Y.A., Zalomaeva, O.V., and Kholdeeva, O.A., *Front. Chem.*, 2019, vol. 7, p. 858:1-14.
26. Suboch, A.N., Cherepanova, S.V., Kibis, L.S., Svinitsitskiy, D.A., Stonkus, O.A., Chesnokov, V.V., Romanenko, A.I., Ismagilov, Z.R., and Podyacheva, O.Yu., *Fullerenes, Nanotubes, Carbon Nanostruct.*, 2016, vol. 24, p. 520.
27. Podyacheva, O.Y., Cherepanova, S.V., Romanenko, A.I., Kibis, L.S., Svinitsitskiy, D.A., Boronin, A.I., Stonkus, O.A., Suboch, A.N., Puzynin, A.V., and Ismagilov, Z.R., *Carbon*, 2017, vol. 122, p. 475.
28. de Correa, C.M., *J. Mol. Catal. A: Chem.*, 2002, vol. 185, nos. 1-2, p. 269.
29. Chizari, K., Janowska, I., Houille, M., Florea, I., Ersen, O., Romero, T., Bernhardt, P., Ledoux, M.J., and Pham-Huu, C., *Appl. Catal., A*, 2010, vol. 380, p. 72.
30. Kumar, K.V., Preuss, K., Guo, Z.X., and Titirici, M.M., *J. Phys. Chem. C*, 2016, vol. 120, p. 18167.
31. Xu, J., Wu, F., Jiang, Q., and Li, Y.-X., *Catal. Sci. Technol.*, 2015, vol. 5, p. 447.
32. Clerici, M. G., *Kinet. Catal.*, 2015, vol. 56, no. 4, p. 450.
33. Esipovich, A.L., Belousov, A.S., Kanakov, E.A., Mironova, V.Yu., Rogozhin, A.E., Danov, S.M., Vorotyntsev, A.V., and Makarov, D.A., *Kinet. Catal.*, 2019, vol. 16, p. 62.
34. Kholdeeva, O.A. and Trukhan, N.N., *Russ. Chem. Rev.* 2006, vol. 75, no. 5, p. 411.
35. Bonon, A.J., Mandelli, D., Kholdeeva, O.A., Barmatova, M.V., Kozlov, Y.N., and Shul'pin, G.B., *Appl. Catal., A*, 2009, vol. 365, no. 1, p. 96.

*Translated by V. Makhlyarchuk*